Two-component model description of Bose-Einstein correlations in *pp* collisions at 13 TeV measured by the CMS Collaboration at the LHC

Takuya Mizoguchi,[1] Seiji Matsumoto,[2] and Minoru Biyajima[3]

[1]*National Institute of Technology, Toba College, Toba 517-8501, Japan*
[2]*School of General Education, Shinshu University, Matsumoto 390-8621, Japan*
[3]*Department of Physics, Shinshu University, Matsumoto 390-8621, Japan*

(Received 31 March 2023; accepted 29 August 2023; published 18 September 2023)

Using the two-component model, we analyze Bose-Einstein correlations in pp collisions at the center-of-mass energy of 13 TeV, measured by the CMS Collaboration at the LHC, and compare results with the τ model. We utilize data described by the double ratios with an average pair transverse momentum $0\ \mathrm{GeV} \le k_T \le 1.0\ \mathrm{GeV}$ and six intervals described by the reconstructed charged-particle multiplicity as $N_{\mathrm{trk}}^{\mathrm{offline}}$. The estimated ranges are 1–4 fm for the magnitude of extension of emitting source expressed by the exponential function $\exp(-RQ)$ and 0.4–0.5 fm for that by the Gaussian distribution $\exp(-(RQ)^2))$, respectively. Moreover, we estimate the upper limits of the 3-pion BEC to test the two-component model and investigate the role of the long-range correlation. Analyses of data at 7 TeV are added for comparisons with results at 13 TeV.

DOI: 10.1103/PhysRevD.108.056014

I. INTRODUCTION

This article investigates the Bose-Einstein correlations (BEC) described by double ratios (DRs) in pp collisions at the center-of-mass energy 13 TeV, obtained by the CMS Collaboration at the LHC [1]. The DR is defined by two single ratios (SRs), i.e., $C_2^{\mathrm{data}} = N^{(2+:2-)}/N^{(+-)}$ and $C_2^{\mathrm{MC}} = N_{\mathrm{MC}}^{(2+:2-)}/N_{\mathrm{MC}}^{(+-)}$, where Ns mean the number of events in data and the Monte Carlo simulation. The suffixes $(2+:2-)$ and $(+-)$ mean the charge combinations. Therein, CMS Collaboration only reports $\chi^2/\mathrm{n.d.f.}$ (number of degrees of freedom) values obtained using the τ model. Here, we analyze the DRs at an average pair-transverse momentum $0\ \mathrm{GeV} \le k_T \le 1.0\ \mathrm{GeV}$ $(k_T = |\mathbf{p}_{T,1} + \mathbf{p}_{T,2}|/2)$, and six intervals expressed by means of constraint $a \le N_{\mathrm{trk}}^{\mathrm{offline}} \le b$ as illustrated in Fig. 1. The formula used in the CMS analysis [2] is

$$F_\tau = C[1 + \lambda\cos((r_0Q)^2 + \tan(\alpha_\tau\pi/4)(Qr)^{\alpha_\tau})e^{-(Qr)^{\alpha_\tau}}] \times (1+\delta Q), \tag{1}$$

where λ, r_0, r, and α_τ are parameters introduced in the stable distribution based on stochastic theory, namely the degree of coherence, two interaction ranges, and the characteristic index, respectively (see, also Refs. [3,4]). $Q = \sqrt{-(p_1 - p_2)^2}$ is the magnitude of the 4-momentum transfer between two pions. The last term $(1+\delta Q)$ is named the long-range correlation with the index (linear) [$\mathrm{LRC}_{(\mathrm{linear})}$]. Our estimated values are presented in Table I.

Because estimated values of all parameters by the τ model, i.e., Eq. (1), have not been presented in Ref. [1], it is difficult to draw physical picture through the analyses of BEC in pp collisions at 13 TeV. Thus for this aim, we present them in Table I. Table I shows that the $\chi^2/\mathrm{n.d.f.}$ values obtained from our analysis are consistent with those reported by the CMS Collaboration [1]. In other words, through concrete figures in Table I, we are able to consider physical picture based on the τ model.

As indicated in Table I, the interaction ranges of the Levy-type form $[e^{-(Qr)^{\alpha_\tau}}]$ increase as the interval containing $N_{\mathrm{trk}}^{\mathrm{offline}}$ increases. The estimated values $r = 20 \sim 50$ fm appear large for pp collisions at 13 TeV.

This paper also investigates this issue from a different perspective, focusing on the collision mechanism. Three processes occur in collisions at the LHC [5–9]; the non-diffractive dissociation (ND), the single-diffractive dissociation (SD), and the double-diffractive dissociation (DD). BEC are related to the chaotic components of particle production. Since the contribution from the DD is Poissonian [9], there is no effect to the BEC. Thus, we calculated the following two-component model correlation function [9,10] (see also empirical Refs. [11–13]),

---

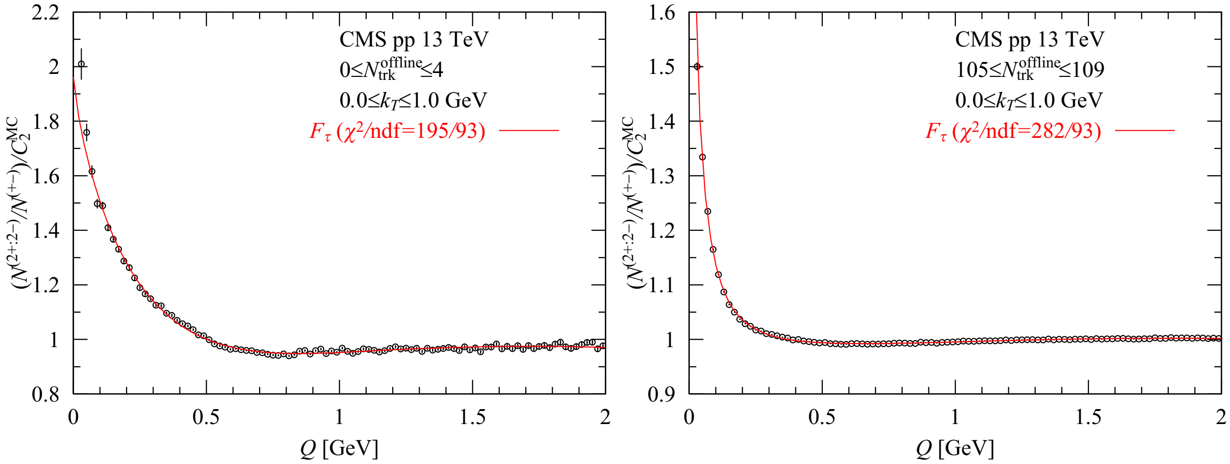

FIG. 1. Fit to the BEC measurements by CMS in pp collisions at 13 TeV by Eq. (1). $C_2^{\rm MC} \equiv N_{\rm MC}^{(2+:2-)}/N_{\rm MC}^{(+-)}$, where $N_{\rm MC}$ means the numbers of the same charged and opposite charged pairs recorded in MC simulations.

$$\mathrm{CF_{II}} = 1 + \lambda_1 E_{\mathrm{BE}_1} + \lambda_2 E_{\mathrm{BE}_2}. \tag{2}$$

The exchange function is the Fourier transform of the space-time region emitting bosons (mainly pion) with overlapping wave functions. For the exchange functions E_{BE_1} and E_{BE_2}, we assign the following two functions [14],

$$\exp(-R_1 Q) \quad \text{and} \quad \exp\left(-(R_2 Q)^2\right) \tag{3}$$

characterizing the exponential and Gaussian type of BEC. Thus, R_1 and R_2 mean the extensions of the sources [14]. Regarding the two kinds of exchange functions, see also the different approach [15].

Moreover, we discuss the LRCs below. Three decades ago, the OPAL Collaboration [16] adopted $\mathrm{LRC_{(OPAL)}} = c(1 + \delta Q + \varepsilon Q^2)$ to improve the linear form $\mathrm{LRC_{(linear)}} = C(1 + \delta Q)$. Recently, we proposed the inverse power series form, $\mathrm{LRC_{(p.s.)}} = C/[1 - \alpha Q \exp(\beta Q)]$ [17], because the number of parameters (α and β) is the same as the $\mathrm{LRC_{(OPAL)}}$s, and it converges to C as Q is large. Taking into account of those investigations and mathematical descriptions shown in Ref. [1], i.e., the distribution of opposite-charged pion pair $N^{(+-)} = C[1 + a \exp(-bQ^2)]$ and so on, we propose the following form:

$$\mathrm{LRC_{(Gauss)}} = \frac{C}{1 + \alpha \exp(-\beta Q^2)}. \tag{4}$$

This function converges to C as Q is large and behaves as $C[1 - \alpha(1 - \beta Q^2) + \cdots]$, Q being small. In Table II, we compare our approach with the formulas shown in Ref. [1].

In the second section, we analyze the BEC at 13 TeV using Eqs. (2)–(4). In the third section, we present our predictions for 3-pion BEC using the two-component model. In the final section, we provide concluding remarks. Appendix A presents an analysis of BEC at 13 TeV using the τ model with Eq. (4). In Appendix B, we reanalyze the CMS BEC at 0.9 TeV and 7 TeV utilizing Eq. (4), because in previous works [9,10], we used $\mathrm{LRC_{(linear)}} = C(1 + \delta Q)$. Therein, to study the k_T dependence of extensions R_1 and R_2's, we analyzed the

TABLE I. Fit parameters to the CMS BEC measurements in pp collisions at 13 TeV at 0.0 GeV $\leq k_T \leq$ 1.0 GeV by Eq. (1). δ values are estimated (top to bottom); -0.016 ± 0.004, 0.03 ± 0.01, 0.005 ± 0.005, $(-1.2 \pm 0.1) \times 10^{-3}$, $(1.3 \pm 0.2) \times 10^{-3}$, and 0.002 ± 0.001.

$N_{\rm trk}^{\rm offline}$	r_0 (fm)	r (fm)	λ	α_τ	χ^2/n.d.f.	χ^2(CMS)
0–4	0.139 ± 0.021	0.93 ± 0.06	0.96 ± 0.05	0.781 ± 0.026	195/93	195
10–12	0.244 ± 0.004	9.08 ± 1.40	2.43 ± 0.23	0.420 ± 0.013	140/93	140
31–33	0.232 ± 0.005	21.8 ± 4.0	3.36 ± 0.37	0.377 ± 0.011	135/93	135
80–84	0.224 ± 0.001	43.7 ± 2.5	4.48 ± 0.15	0.351 ± 0.003	899/93	902
105–109	0.216 ± 0.003	47.0 ± 5.2	4.71 ± 0.31	0.352 ± 0.005	282/93	281
130–250	0.228 ± 0.013	53.3 ± 19.9	5.32 ± 1.27	0.353 ± 0.020	84.5/93	84

TABLE II. Comparison of our approach with formulas utilized by CMS Collaboration [1].

	Formulas	cf.
Our approach	$\mathrm{CF_{II}} \times \mathrm{LRC}$ where $\mathrm{LRC_{(Exp)}} = \frac{1}{1+\alpha e^{-\beta Q}}$, or $\mathrm{LRC_{(Gauss)}} = \frac{1}{1+\alpha e^{-\beta Q^2}}$.	(1) $\mathrm{CF_{II}}$ is reflecting to three kinds of multiplicity distributions of the ND, SD, and DD in pp collisions. (2) Through the generalization of $\mathrm{LRC_{(OPAL)}} = 1 + \delta Q + \varepsilon Q^2$ in e^+e^- annihilation at Z^0-pole [16], we obtained $\mathrm{LRC_{(Exp)}}$ [17]. (3) Referring to mathematical descriptions on F_{2N} and F_{2D} in Ref [1], $\mathrm{LRC_{(Gauss)}}$ is proposed for pp collisions.
CMS	(1) Distributions $N^{(2+:2-)}$, $N^{(+-)}$, $N_{\mathrm{MC}}^{(2+:2-)}$ and $N_{\mathrm{MC}}^{(+-)}$ are assumed as follows: $\mathrm{CF_I} \cdot C(1+ae^{-bQ^2})$, $C'(1+a'e^{-b'Q^2})$, $C_M(1+a_Me^{-b_MQ^2})$, and $C'_M(1+a'_Me^{-b'_MQ^2})$, respectively. (2) SRs $F_{2N} = N^{(2+:2-)}/N^{(+-)}$ and $F_{2D} = N_{\mathrm{MC}}^{(2+:2-)}/N_{\mathrm{MC}}^{(+-)}$ are used for analysis of data of DR by the ratio F_{2N}/F_{2D}. (3) τ model is also used for data of DR.	(1) $\mathrm{CF_I} = 1 + \lambda E_{\mathrm{BE}}$, where $E_{\mathrm{BE}} = \exp(-RQ)$ [1]. (2) Provided that $N_{\mathrm{MC}}^{(+-)} \cong N^{(+-)}$ and the cross term $(\lambda a E_{\mathrm{BE}} \cdot e^{-bQ^2})$ is small, we obtain $\frac{F_{2N}}{F_{2D}} \cong \frac{\mathrm{CF_I}\times(1+ae^{-bQ^2})}{1+a_Me^{-b_MQ^2}} \cong \mathrm{CF_{II}} \times \mathrm{LRC_{(Gauss)}}$. Thus, α and β in Eq. (4) are approximately identified with a_M and b_M describing the Monte Carlo events in F_{2D}, respectively. (3) Monte Carlo events are calculated with PYTHIA 6.Z2* tune. See Fig. 1 in Ref. [1]. (4) Notice that $\langle n\rangle_{\mathrm{SD}}$ by PYTHIA 6 is smaller than that by PYTHIA 8 at 7 TeV and 8 TeV [5–7]. (5) Corrections to empirical data are performed by PYTHIA 8 with CUETP8M1 tune for MB (minimum bias) and 4C tune for high multiplicity (HM) events, respectively. (6) Reconstructed tracks with $\lvert\eta\rvert < 2.4$ and $p_T > 0.2$ GeV are required. The extrapolation method (0 GeV $< k_T <$ 0.2 GeV) is used in data on BEC.

data on BEC at 7 TeV by Eqs. (2)–(4), because in Ref. [2] data with several intervals are presented.

II. ANALYSIS OF BEC AT 13 TeV USING EQS. (2)–(4)

Considering the results of the CMS BEC at 7 TeV in Ref. [9], we assume a combination of exponential function and Gaussian distribution, as this combination has shown a valuable role. Moreover, it is worthwhile mentioning that Shimoda *et al.* in Ref. [14] investigated several possible distributions for E_{BE}s. Our results are presented in Fig. 2 and Table III. We observe extraordinary behaviors in the two intervals, $0 \le N_{\mathrm{trk}}^{\mathrm{offline}} \le 4$ and $10 \le N_{\mathrm{trk}}^{\mathrm{offline}} \le 12$, of the LRC shown in Fig. 3.

As indicated by Fig. 2 and Table III, the two-component model with Eqs. (2)–(4) effectively characterizes three intervals; $31 \le N_{\mathrm{trk}}^{\mathrm{offline}} \le 33$, $80 \le N_{\mathrm{trk}}^{\mathrm{offline}} \le 84$, and $105 \le N_{\mathrm{trk}}^{\mathrm{offline}} \le 109$.

Among the six intervals shown in Fig. 3, the red (solid) line and green (dashed) line appear to be exceptional. They are probably related to the normalization factors (0.980 ± 0.004 and 1.031 ± 0.001). In other words, in those regions there is very small freedom or noise which cannot be described by Eqs. (2)–(4).

III. TEST OF THE TWO-COMPONENT MODEL FOR 3-PION BEC

Here, we investigate the 3-pion BEC using the two-component model. Since there is currently no information from CMS on the multiplicity distribution $P(n)$ at 13 TeV, it is challenging to determine the ratio between the contributions of the first and the second components. We use the diagrams in Fig. 4.

The formula that corresponds to the diagrams in Fig. 4 [18–20] is expressed as

$$F_i^{(3)} = 1.0 + 3\lambda_i E_{\mathrm{BE}_i} + 2(\lambda_i E_{\mathrm{BE}_i})^{3/2}. \tag{5}$$

By assuming an equal weight for the first and the second components, $F_1^{(3)}$ and $F_2^{(3)}$, we obtain the following normalized expression

$$F^{(3+:3-)} = 1.0 + \frac{1}{2}\Big(3\lambda_1 E_{\mathrm{BE}_1} + 2(\lambda_1 E_{\mathrm{BE}_1})^{3/2}\Big) + \frac{1}{2}\Big(3\lambda_2 E_{\mathrm{BE}_2} + 2(\lambda_2 E_{\mathrm{BE}_2})^{3/2}\Big), \tag{6}$$

where λ_1, λ_2, R_1, and R_2 are fixed by using the numerical values in Table III. Typical figures are presented in Fig. 5. We could calculate the ratio if the CMS Collaboration

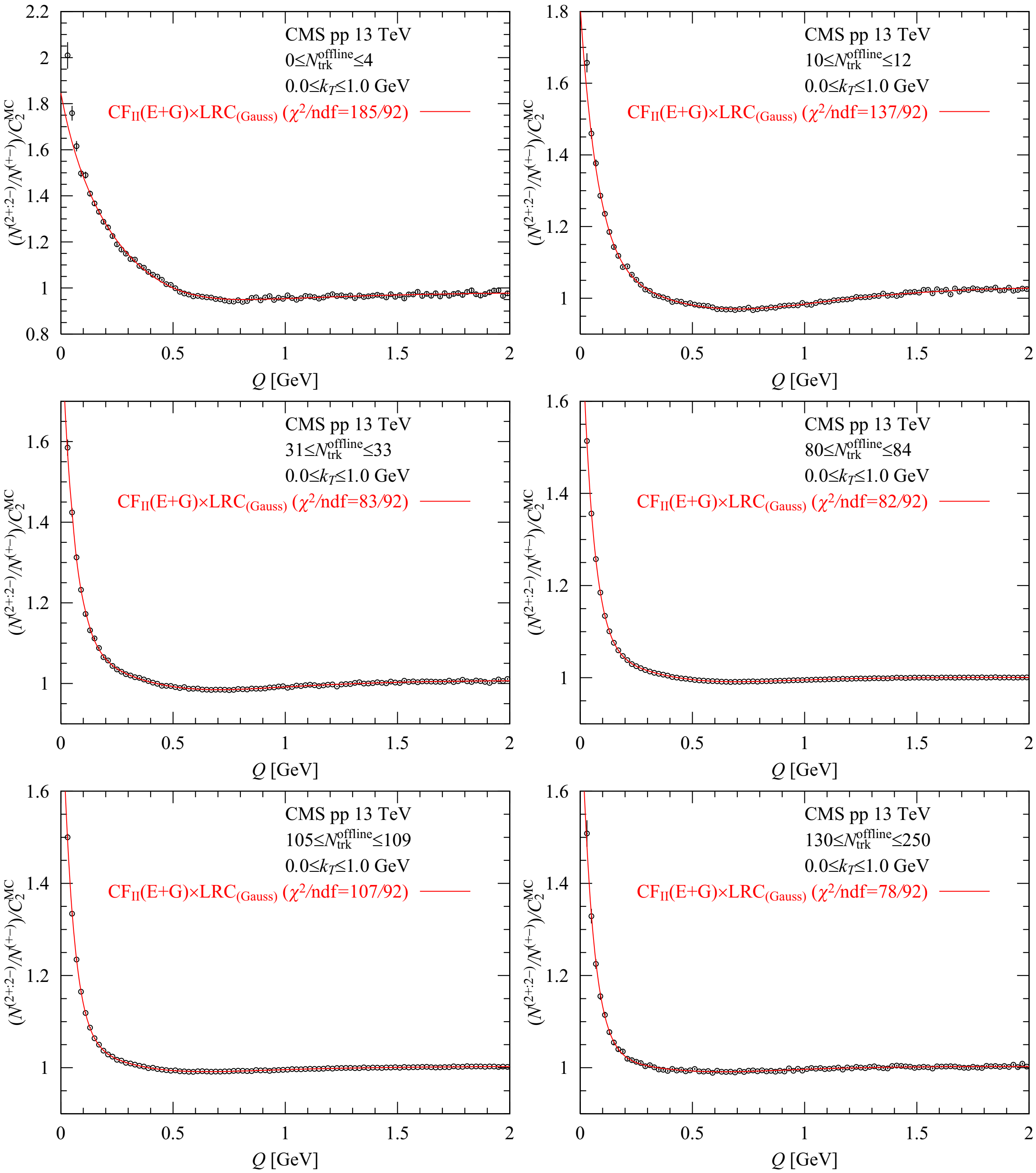

FIG. 2. Fit to the BEC measurements by CMS in pp collisions at 13 TeV by Eqs. (2)–(4).

reports the multiplicity distributions $P(n)$ [2], as this would allow us to understand the ensemble property of the BEC through the multiplicity distribution. It is worth noting that the ATLAS Collaboration has already observed the multiplicity distributions $P(n)$ [21] and BEC [22] considered in [23].

In the near future, we may be able to further test the two-component model when the CMS Collaboration analyzes the 3-pion BEC. If we observe the same extensions as in Fig. 2, we could conclude that the two-component model is a viable approach.

IV. CONCLUDING REMARKS

(C1) Our analysis of CMS BEC at 13 TeV using the τ model with Eq. (1) confirms the applicability

TABLE III. Fit parameters of the CMS measurements of BEC in pp collisions at 13 TeV (0.0 GeV $\le k_T \le$ 1.0 GeV) by Eqs. (2)–(4). Three constraints are used; $\lambda_1 \le 1.0$, $\lambda_2 \le 1.0$, and $\lambda_1 + \lambda_2 \le 1.0$. The p-values for the three intervals $31 \le N_{\rm trk}^{\rm offline} \le 33$, $80 \le N_{\rm trk}^{\rm offline} \le 84$, and $130 \le N_{\rm trk}^{\rm offline} \le 250$ are 73.0%, 77.3%, and 85.3%, respectively. C (top to bottom): 0.980 ± 0.004, 1.031 ± 0.001, 1.007 ± 0.001, $1.001 \pm 1 \times 10^{-4}$, $1.003 \pm 2 \times 10^{-4}$, 1.003 ± 0.001, 0.972 ± 0.002, 1.028 ± 0.002, and 1.007 ± 0.001.

$N_{\rm trk}^{\rm offline}$	R_1 (fm)	R_2 (fm)	λ_1	λ_2	α	β (GeV^{-2})	χ^2/n.d.f.
0–4	1.57 ± 0.15	0.51 ± 0.01	0.680 ± 0.034	0.320 ± 0.034	0.062 ± 0.006	0.79 ± 0.18	185.4/92
10–12	2.40 ± 0.07	0.39 ± 0.02	0.865 ± 0.007	0.135 ± 0.007	0.136 ± 0.009	0.99 ± 0.07	137.1/92
31–33	3.37 ± 0.07	0.48 ± 0.02	0.910 ± 0.004	0.090 ± 0.004	0.048 ± 0.004	1.06 ± 0.12	83.3/92
80–84	3.76 ± 0.03	0.49 ± 0.01	0.866 ± 0.007	0.061 ± 0.001	0.026 ± 0.001	1.53 ± 0.06	81.6/92
105–109	4.02 ± 0.06	0.57 ± 0.01	0.867 ± 0.149	0.050 ± 0.002	0.020 ± 0.001	1.06 ± 0.07	107.0/92
130–250	3.79 ± 0.22	0.46 ± 0.09	0.857 ± 0.051	0.040 ± 0.011	0.030 ± 0.014	1.54 ± 0.51	77.6/92
Note: When no constraint is applied for λ_1 and λ_2, we obtain the following figures:							
0–4	2.76 ± 0.30	0.49 ± 0.02	1.085 ± 0.083	0.477 ± 0.052	0.112 ± 0.051	1.78 ± 0.57	126.6/92
10–12	2.50 ± 0.09	0.37 ± 0.02	0.947 ± 0.033	0.168 ± 0.025	0.165 ± 0.028	1.17 ± 0.13	128.8/92
31–33	3.43 ± 0.11	0.48 ± 0.02	0.928 ± 0.029	0.092 ± 0.004	0.048 ± 0.004	1.06 ± 0.12	83.0/92

of this model. This is evidenced by the values of χ^2 in Table I.

(C2) As portrayed in Table I, the interaction ranges r in the Lévy-type expression $e^{-(Qr)^{\alpha_\tau}}$ increase as the range of the interval $N_{\rm trk}^{\rm offline}$ increases. However, it appears that the interaction ranges from 30 to 50 fm are large in pp collisions at 13 TeV.

(C3) To gain a better understanding of the results obtained from the τ model, we have analyzed the BEC using the τ model with Eq. (4). This has led to improved estimations, as shown in Appendix A.

(C4) We look forward to future analyses by the CMS Collaboration of the multiplicity distributions and the third-order BEC at 13 TeV. Concerning with the Monte Carlo simulations, see Refs. [5–7].

Hereafter, we summarize the results of the two-component model using Eqs. (2)–(4).

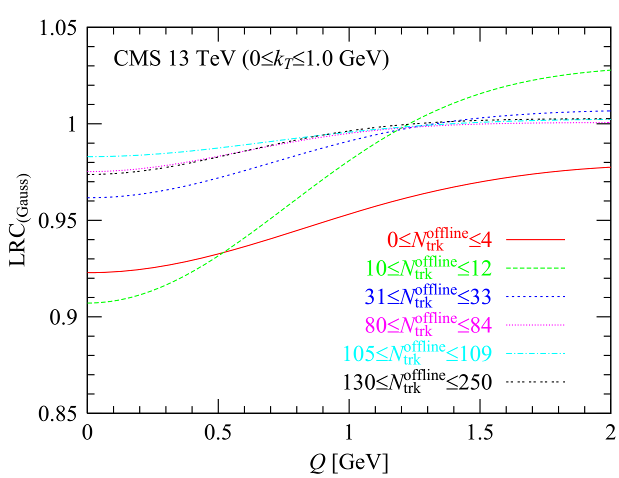

FIG. 3. The long-range correlations (LRCs), see Eq. (4) for six intervals.

(C5) In Table II, we mentioned how to propose LRC$_{\rm (Gauss)}$, i.e., Eq. (4). To investigate the remarks mentioned in *C2)* above using the two-component model, we utilized Eqs. (2)–(4). Our results are presented in Table III. The large extensions are approximately 4 fm, and they appear to be reasonable.

(C6) Furthermore, to test the availability of the two-component model, we calculated the 3-pion BEC by making use of the estimated values and diagrams presented in Fig. 4. Interestingly, as $N_{\rm trk}^{\rm offline}$ increases, the 3-pion BEC rapidly decreases, due to the changes in the extension R_1 (1–4 fm). Moreover, the intercepts at $Q = 0.0$ GeV are about 3.0, providing the equal weight.

(C7) To investigate the role of the LRC$_{\rm (Gauss)}$, i.e., Eq. (4), we reanalyzed the BEC at 0.9 TeV and 7 TeV, with the results presented in Appendix B. The estimated χ^2 values became smaller than those of LRC$_{\rm (linear)}$ [9].

(C8) As portrayed in Table III, the BEC in the intervals $0 \le N_{\rm trk}^{\rm offline} \le 4$ and $10 \le N_{\rm trk}^{\rm offline} \le 12$ cannot be analyzed with better χ^2 values. A more complicated model may be necessary.

(C9) From Table III, we can observe behaviors of R_1s and R_2s at 13 TeV in Fig. 6 (left panel). The larger extension R_1s seem to be saturated at larger $N_{\rm trk}^{\rm offline}$. To confirm that, of course, more data are needed.

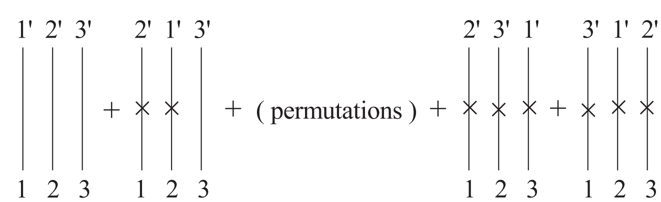

FIG. 4. Diagrams for the third-order BEC. The matrix indicates the exchange of identical pions.

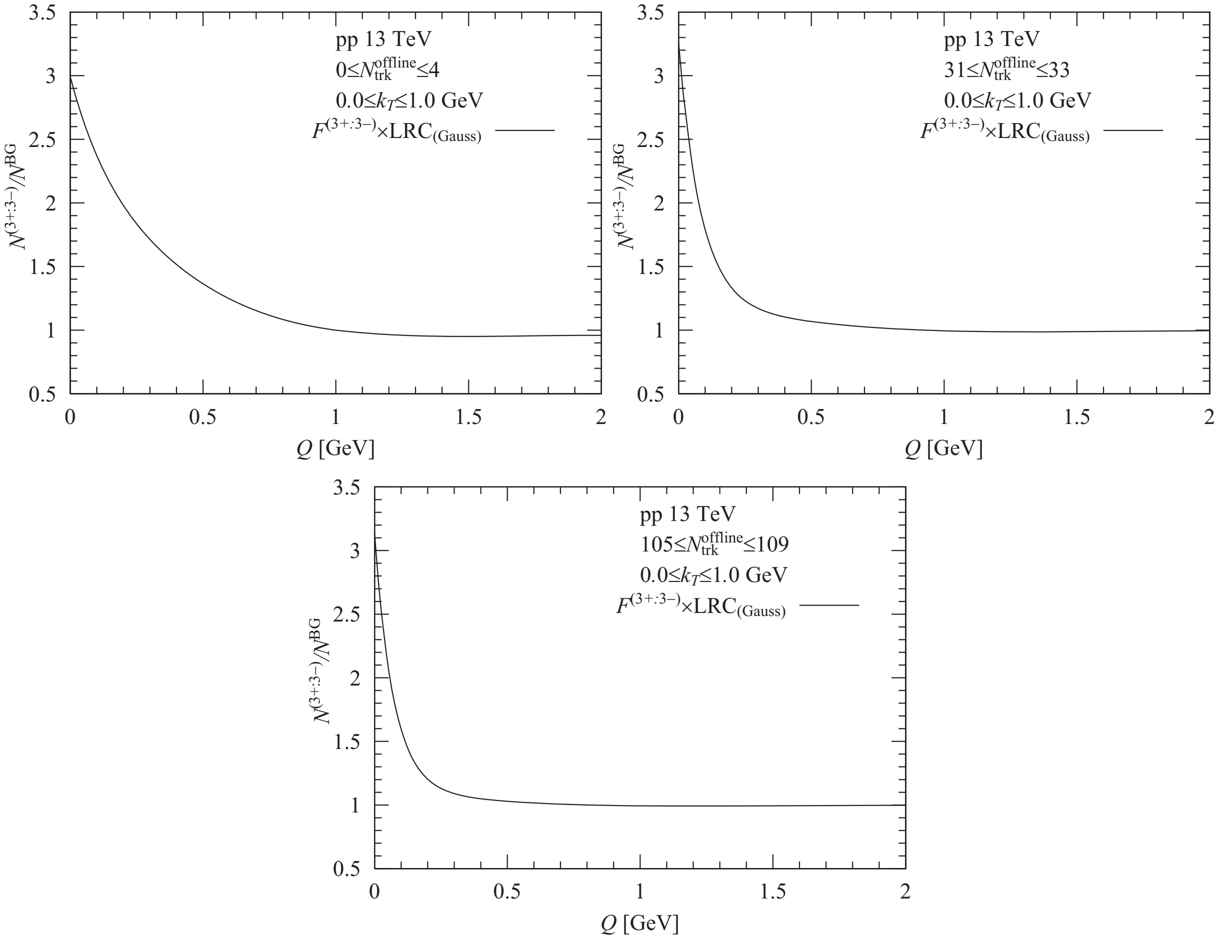

FIG. 5. Prediction of upper limit of the 3π BEC in pp collisions at 13 TeV by means of Eq. (6) with Eqs. (2)–(4). $N^{(\mathrm{BG})}$ means $N_{\mathrm{MC}}^{(3+:3-)}$, because of no BECs in the Monte Carlo events.

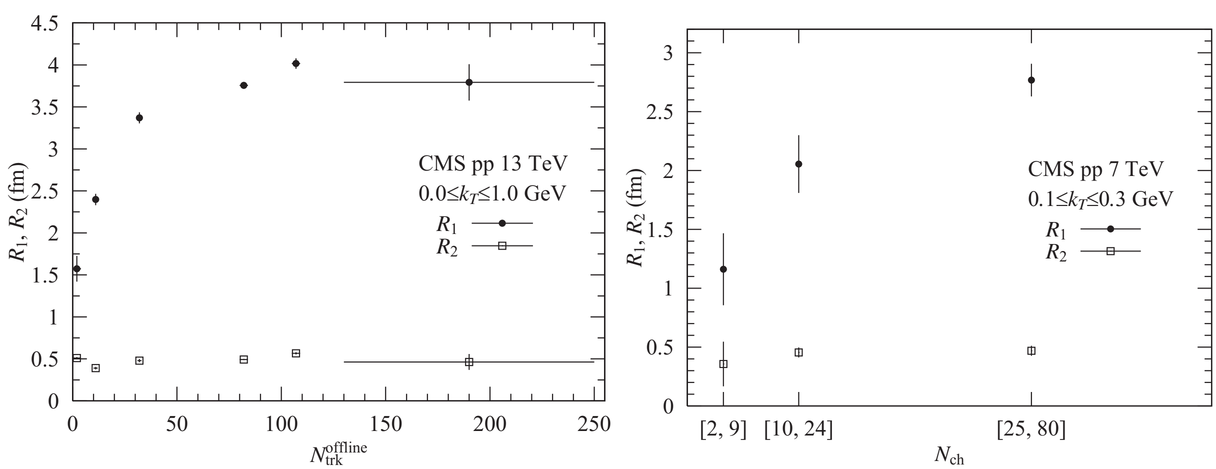

FIG. 6. Behaviors of R_1s and R_2s at 13 TeV and 7 TeV are shown from Tables III and VI. The smaller extension R_2s are almost the constants.

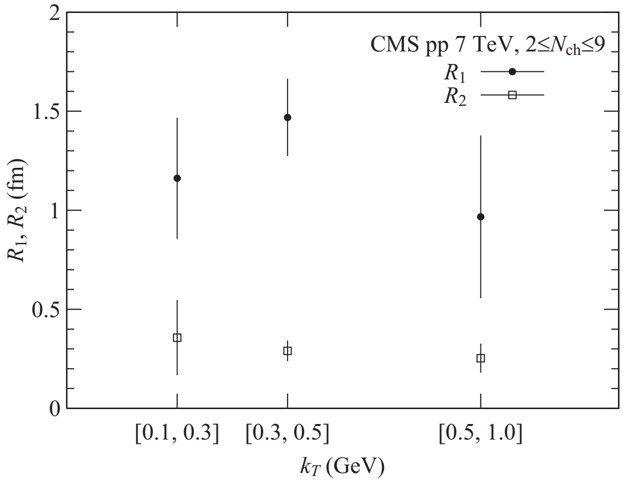

FIG. 7. Behaviors of R_1s and R_2s at 7 TeV are shown from Table VI. The smaller extension R_2 decreases as k_T increases. See an interesting paper [24]; therein the latter behavior is predicted.

We also analyzed the data at 7 TeV with the constraint 0.1 GeV $\le k_T \le 0.3$ GeV (fixed) and three intervals $2 \le N_{\rm ch} \le 9$, $10 \le N_{\rm ch} \le 24$ and $25 \le N_{\rm ch} \le 80$. We observe that R_1s increase and that R_2s are almost constants in Fig. 12 in Appendix B.

(C10) Moreover, Fig. 7 shows an interesting behavior. Observe Fig. 12 and Table VI in Appendix B, where data at 7 TeV with the constraints $0.1 \le k_T \le 0.3$, $0.3 \le k_T \le 0.5$, and 0.5 GeV $\le k_T \le 1.0$ GeV and $2 \le N_{\rm ch} \le 9$ (fixed) are analyzed. See also consideration for two kinds of extensions mentioned in Refs. [15,24]. Their arguments are quantitatively supported.

Provided that data on BEC at 13 TeV with $0.1(0.2) \le k_T \le 0.3$, $0.3 \le k_T \le 0.5$, and 0.5 GeV $\le k_T \le 1.0$ GeV with $2 \le N_{\rm ch} \le 9$ (fixed) were reported, we could obtain an interesting information based on comparisons of those expected data with Fig. 7.

ACKNOWLEDGMENTS

One of the authors (M. B.) would like to thank his colleagues at the Department of Physics, Shinshu University.

APPENDIX A: ANALYSIS OF BEC AT 13 TeV USING THE τ MODEL WITH EQ. (4)

We are interested in the influence of Eq. (4) on the τ model. To investigate this, we reanalyzed the BEC using the following formula

$$F_{\tau\text{-Gauss}} = [1 + \lambda \cos((r_0 Q)^2 + \tan(\alpha_\tau \pi/4)(Qr)^{\alpha_\tau}) e^{-(Qr)^{\alpha_\tau}}] \times {\rm LRC}_{\rm (Gauss)}. \tag{A1}$$

Our findings are presented in Fig. 8 and Table IV. It can be seen that the interaction-range r values are smaller than 10 fm.

As illustrated in Fig. 9, three LRC's appear to be various. Therein the behavior of LRC for $0 \le N_{\rm trk}^{\rm offline} \le 4$ is related to the negative α. For the sake of reference, we demonstrate the effective degree of coherence in the τ model

$$\lambda_{\rm eff} = \lambda \cos((r_0 Q)^2 + \tan(\alpha_\tau \pi/4)(Qr)^{\alpha_\tau})$$

in Fig. 9. By making use of $\lambda_{\rm eff}$s and LRCs, we can estimate the intercepts at $Q = 0.0$ GeV, which are shown in Fig. 8.

APPENDIX B: REANALYSIS OF CMS BEC AT 0.9 TeV AND 7 TeV [2] BY LRC, EXPRESSED BY EQ. (4)

We examined the changes in the values of χ^2 when ${\rm LRC}_{\rm (linear)}$ was replaced with Eq. (4) in the reanalysis of BEC at 0.9 TeV and 7 TeV [2]. Our new results obtained using Eq. (4) are presented in Fig. 10 and in Table V and compared with those obtained elsewhere [9], where the linear form for the LRC $= C(1 + \delta Q)$ was used. These results are also shown in Table V. We show the LRCs in Fig. 11.

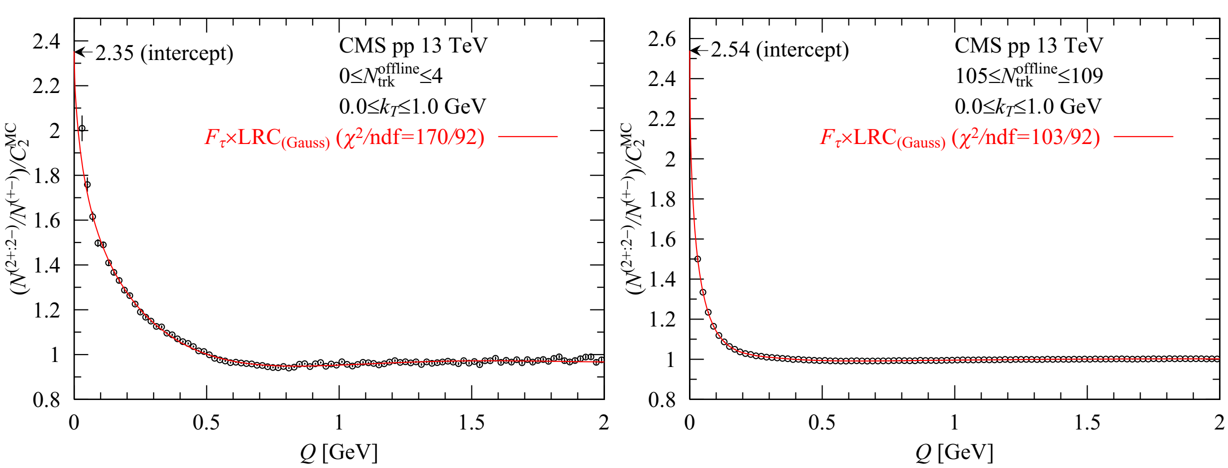

FIG. 8. Fit to the BEC measurements by CMS in pp collisions at 13 TeV by Eq. (A1) with Eq. (4).

TABLE IV. Fit parameters of the CMS measurements of BEC in pp collisions at 13 TeV (0.0 GeV $\le k_T \le$ 1.0 GeV) using the τ model with Eq. (4).

$N_{\rm trk}^{\rm offline}$	r_0 (fm)	r (fm)	λ	α_τ	α	β	χ^2/n.d.f.
0–4	0.22 ± 0.02	2.12 ± 0.52	1.02 ± 0.12	0.595 ± 0.047	-0.169 ± 0.017	5.60 ± 0.49	169.6/92
10–12	0.25 ± 0.01	9.89 ± 1.69	2.49 ± 0.25	0.417 ± 0.014	0.099 ± 0.060	0.17 ± 0.13	138.7/92
31–33	0.16 ± 0.01	3.27 ± 0.45	1.76 ± 0.10	0.566 ± 0.022	0.177 ± 0.024	19.86 ± 1.02	85.9/92
80–84	0.00	3.76 ± 0.06	1.65 ± 0.02	0.566 ± 0.002	0.159 ± 0.003	23.83 ± 0.31	166.2/92
105–109	0.13 ± 0.01	5.61 ± 0.54	1.84 ± 0.08	0.517 ± 0.012	0.119 ± 0.010	25.48 ± 0.73	103.1/92
130–250	0.18 ± 0.02	9.02 ± 3.43	2.18 ± 0.42	0.468 ± 0.037	0.076 ± 0.024	21.63 ± 3.39	78.5/92

It can be said that the Gaussian distribution of the LRC in the two-component model is better than that of the linear form, because the LRC$_{\rm (Gauss)}$ converges to 1.0 in the region of $Q \ge 2.0$ GeV. The reason is as follows: The emitting source functions and/or the LRCs in the Euclidean space ($Q' = \sqrt{(\mathbf{p}_1 - \mathbf{p}_2)^2 + (E_1 - E_2)^2}$ and $\xi' = \sqrt{(\mathbf{r}_1 - \mathbf{r}_2)^2 + (t_1 - t_2)^2}$) are calculated as

$$F_{\rm source}(\xi', R) = \frac{1}{(2\pi)^2 \xi'} \int_0^\infty Q'^2 E_{\rm BE}(Q', R) J_1(Q'\xi') dQ', \tag{B1}$$

where $J_1(Q\xi)$ is the Bessel function. For the LRC, we should replace $E_{\rm BE}$ with (LRC $-$ 1.0) and R with β in Eq. (B1), respectively. In other words, the

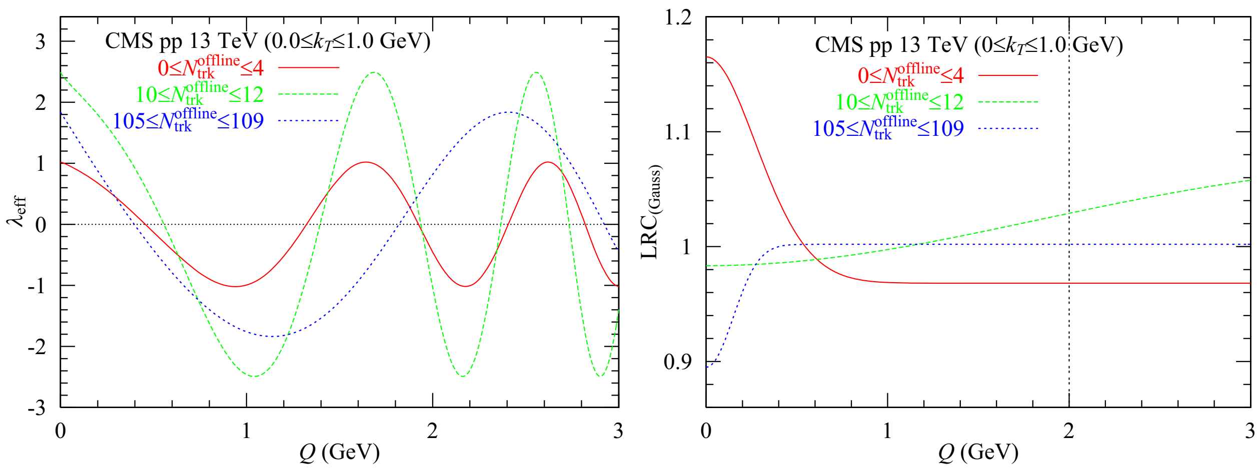

FIG. 9. $\lambda_{\rm eff}$'s and LRCs of BEC measurements by CMS in pp collisions at 13 TeV by Eq. (A1). The vertical line at $Q = 2.0$ GeV represents the effective range of the LRC (0 GeV $\le Q \le$ 2 GeV).

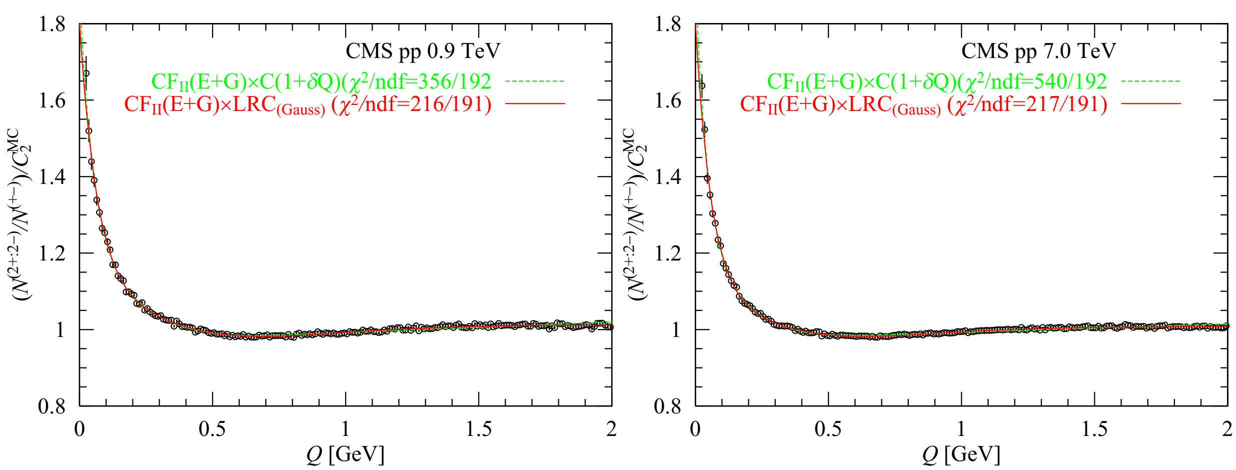

FIG. 10. Fit to the CMS BEC measurements in pp collisions at 0.9 TeV and 7.0 TeV by Eqs. (2)–(4).

TABLE V. Fit parameters of the CMS BEC measurements in pp collisions at 0.9 TeV and 7.0 TeV by Eqs. (2)–(4).

	R_1 (fm)	R_2 (fm)	λ_1	λ_2	δ (GeV^{-1}) or (α, β (GeV^{-2}))	χ^2/n.d.f.
$\sqrt{s} = 0.9$ TeV						
LRC$_{\text{(linear)}}$ [9]	3.37 ± 0.19	0.62 ± 0.01	0.80 ± 0.04	0.14 ± 0.01	0.029 ± 0.001	356/192
Equation (4)	2.83 ± 0.16	0.48 ± 0.03	0.78 ± 0.03	0.13 ± 0.01	$(0.07 \pm 0.01, 1.27 \pm 0.13)$	216/191
$\sqrt{s} = 7$ TeV						
LRC$_{\text{(linear)}}$ [9]	3.88 ± 0.18	0.71 ± 0.01	0.84 ± 0.03	0.12 ± 0.01	0.023 ± 0.001	540/192
Equation (4)	3.13 ± 0.13	0.51 ± 0.02	0.80 ± 0.03	0.10 ± 0.01	$(0.06 \pm 0.01, 1.46 \pm 0.11)$	217/191

$(\text{LRC}_{\text{(Gauss)}} - 1.0) = \sum_{k=1}^{\infty}(-\alpha e^{-\beta Q^2})^k$ is preferable to the $(\text{LRC}_{\text{(linear)}} - 1.0) = \delta Q$, because the former converges, as Q is large. Finally, we should adopt the inverse Wick rotation for ξ' [14,17]; $\xi = \sqrt{(\mathbf{r}_1 - \mathbf{r}_2)^2 - (t_1 - t_2)^2}$.

Moreover, we analyzed data on BEC at 7 TeV with three intervals $(0.1 \le k_T \le 0.3,\ 0.3 \le k_T \le 0.5$ and $0.5\ \text{GeV} \le k_T \le 1.0\ \text{GeV})$ and those for N_{ch} $(2 \le N_{\text{ch}} \le 9,\ 10 \le N_{\text{ch}} \le 24,$ and $24 \le N_{\text{ch}} \le 80)$ in Ref. [2] by means of Eqs. (2)–(4). The smaller extensions with 0.1 GeV $\le k_T \le$ 0.3 GeV are almost constant. This fact is similar to Fig. 6 (left panel). From estimated parameters with the constraint $2 \le N_{\text{ch}} \le 9$ (fixed) in the low column, we see that R_2s are probably decreasing.

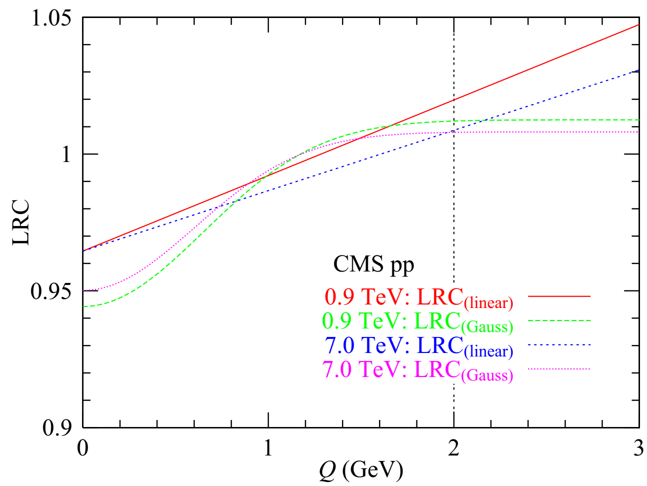

FIG. 11. LRCs by LRC$_{\text{(linear)}}$ [9] and LRC$_{\text{(Gauss)}}$ [Eq. (4)] of CMS BEC measurements in pp collisions at 0.9 TeV and 7.0 TeV are presented. The vertical line at $Q = 2.0$ GeV represents the effective range of the LRC (0 GeV $\le Q \le$ 2 GeV).

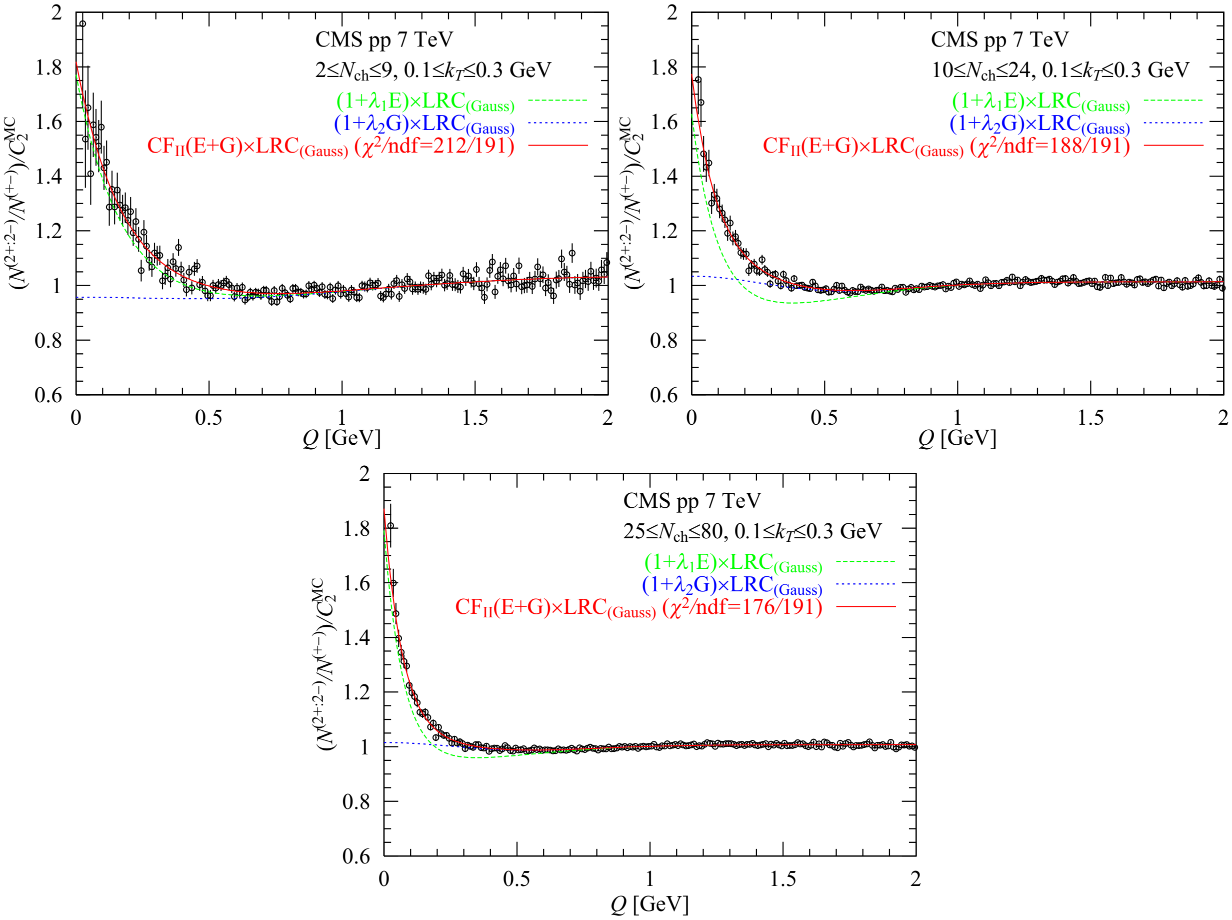

FIG. 12. Fit to the BEC measurements by CMS in pp collisions at 7 TeV with 0.1 GeV $\leq k_T \leq$ 0.3 GeV by Eqs. (2)–(4).

TABLE VI. Fit parameters of the CMS BEC measurements in pp collisions at 7.0 TeV with 0.1 GeV $\leq k_T \leq$ 0.3 GeV and $2 \leq N_{\mathrm{ch}} \leq 9$ by Eqs. (2)–(4) with $0 \leq \lambda_1 \leq 1$ and $\lambda_2 = 1 - \lambda_1$. N_{ch} means the charged particle multiplicity. C (top to bottom): 1.037 ± 0.011, 1.013 ± 0.001, 1.008 ± 0.001, 1.010 ± 0.008, and 1.037 ± 0.011.

	R_1 (fm)	R_2 (fm)	λ_1	λ_2	α	β (GeV^{-2})	χ^2/n.d.f.
$0.1 \leq k_T \leq 0.3$ (fixed)							
$2 \leq N_{\mathrm{ch}} \leq 9$	1.16 ± 0.31	0.36 ± 0.19	0.95 ± 0.10	0.05 ± 0.10	0.14 ± 0.04	0.80 ± 0.28	212/192
$10 \leq N_{\mathrm{ch}} \leq 24$	2.05 ± 0.25	0.46 ± 0.04	0.95 ± 0.10	0.05 ± 0.10	0.14 ± 0.03	2.42 ± 0.24	188/192
$25 \leq N_{\mathrm{ch}} \leq 80$	2.77 ± 0.14	0.47 ± 0.04	0.91 ± 0.02	0.09 ± 0.02	0.08 ± 0.02	2.47 ± 0.26	176/192
$2 \leq N_{\mathrm{ch}} \leq 9$ (fixed)							
$0.1 \leq k_T \leq 0.3$	1.16 ± 0.31	0.36 ± 0.19	0.95 ± 0.10	0.05 ± 0.10	0.14 ± 0.04	0.80 ± 0.28	212/192
$0.3 \leq k_T \leq 0.5$	1.47 ± 0.20	0.29 ± 0.05	0.86 ± 0.03	0.14 ± 0.03	0.15 ± 0.04	0.99 ± 0.23	198/192
$0.5 \leq k_T \leq 1.0$	0.97 ± 0.41	0.25 ± 0.07	0.71 ± 0.10	0.29 ± 0.10	0.43 ± 0.08	1.16 ± 0.32	177/192

[1] A. M. Sirunyan *et al.* (CMS Collaboration), J. High Energy Phys. 03 (2020) 014.

[2] V. Khachatryan *et al.* (CMS Collaboration), J. High Energy Phys. 05 (2011) 029.

[3] H. Takayasu, *Fractals in the Physical Sciences* (Manchester University Press, Manchester and New York, 1990).

[4] K. Itô, *Kakuritsu Katei (Translation from the English language edition, "Stochastic Processes")* (Springer-Verlag, Berlin, Heidelberg, 2004).

[5] S. Navin, Diffraction in ALICE and trigger efficiencies, Report No. CERN-THESIS-2011-378.

[6] ATLAS Collaboration, Charged particle multiplicities in pp interactions for track pT $>$ 100 MeV at sqrts $=$ 0.9 and 7 TeV measured with the ATLAS detector at the LHC, Report No. ATLAS-CONF-2010-046.

[7] W. Lukas, Measurement of charged-particle distributions in proton–proton interactions at $\sqrt{s} = 8$ TeV with the ATLAS detector at the LHC, Report No. CERN-THESIS-2016-420.

[8] I. Zborovský, J. Phys. G **40**, 055005 (2013).

[9] M. Biyajima and T. Mizoguchi, Int. J. Mod. Phys. A **34**, 1950203 (2019).

[10] T. Mizoguchi and M. Biyajima, J. Phys. Soc. Jpn. Conf. Proc. **26**, 031032 (2019).

[11] T. Åkesson *et al.* (Axial Field Spectrometer Collaboration), Z. Phys. C **36**, 517 (1987).

[12] N. M. Agababyan *et al.* (EHS/NA22 Collaboration), Z. Phys. C **59**, 195 (1993).

[13] B. Lorstad, Int. J. Mod. Phys. A **04**, 2861 (1989).

[14] R. Shimoda, M. Biyajima, and N. Suzuki, Prog. Theor. Phys. **89**, 697 (1993).

[15] V. A. Khoze, A. D. Martin, M. G. Ryskin, and V. A. Schegelsky, Eur. Phys. J. C **76**, 193 (2016).

[16] P. D. Acton *et al.* (OPAL Collaboration), Phys. Lett. B **267**, 143 (1991).

[17] T. Mizoguchi, S. Matsumoto, and M. Biyajima, Int. J. Mod. Phys. A **37**, 2250148 (2022).

[18] M. Biyajima, A. Bartl, T. Mizoguchi, O. Terazawa, and N. Suzuki, Prog. Theor. Phys. **84**, 931 (1990); See also **88**, 157 (1992).

[19] N. Suzuki and M. Biyajima, Phys. Rev. C **60**, 034903 (1999).

[20] G. A. Kozlov, O. V. Utyuzh, G. Wilk, and Z. Wlodarczyk, Phys. At. Nucl. **71**, 1502 (2008).

[21] M. Aaboud *et al.* (ATLAS Collaboration), Eur. Phys. J. C **76**, 502 (2016).

[22] G. Aad *et al.* (ATLAS Collaboration), Eur. Phys. J. C **82**, 608 (2022).

[23] M. Biyajima, T. Mizoguchi, and S. Matsumoto (to be published).

[24] V. A. Schegelsky, A. D. Martin, M. G. Ryskin, and V. A. Khoze, Phys. Lett. B **703**, 288 (2011).